This article has been accepted for publication in a future issue of this journal, but has not been fully edited. Content may change prior to final publication. Citation information: DOI 10.1109/TSP.2020.2983644, IEEE Transactions on Signal Processing

Differential and Weighted Slepian Concentration Problems on the Sphere

Wajeeha Nafees, *Student Member, IEEE*, Zubair Khalid, *Member, IEEE* and Rodney A. Kennedy, *Fellow, IEEE*

***Abstract*—In this work, we present a generalized formulation of the Slepian concentration problem on the sphere for finding band-limited functions with an optimal concentration in the spatial domain. By introducing weighting functions in the formulation of classical Slepian concentration problem and assigning different values to these weighting functions, we present two variants of the concentration problem namely the *differential* and the *weighted* Slepian concentration problem. In the differential Slepian concentration problem, we consider two regions on the sphere and find band-limited functions such that the energy is maximized in one region at the expense of the energy in the other region. We propose non-negative weighting using a spatial window function to formulate and solve the weighted Slepian concentration problem. Each problem can be solved by formulating it in the harmonic domain as an eigenvalue problem, the solution of which yields eigenfunctions that serve as alternative basis functions for the representation of band-limited signals and are referred to as Slepian functions. We also present and analyse the properties of the Slepian functions. To support the applications in acoustics and cosmology, we also provide a demonstration for the use of the proposed Slepian functions for the robust signal modeling and the estimation of the energy spectrum of red and white stochastic processes on the sphere.**

***Index Terms*—Slepian concentration problem, spatial-spectral concentration problem, spherical signals, spherical harmonic transform (SHT), unit sphere, band-limited signals, spectral analysis.**

EDICS: MDS-ALGO, DSP-TRSF.

I. Introduction

According to the uncertainty principle, it is not possible for a signal to have finite support in the time domain and frequency domain simultaneously. In other words, a function that is limited in the spatial (or temporal) domain has an infinite support in the spectral (or frequency) domain and vice versa. However, it is possible to find the maximal concentration of a function in a particular region of one domain while it is strictly limited in the other domain. The problem of finding functions that are optimally concentrated in spatial and spectral domains simultaneously is known as the Slepian concentration problem, which was first proposed in a series of classical papers [1]–[4] for the one-dimensional time-frequency domain. The orthogonal family of functions, or data tapers, that arise thereby are known as the Prolate Spheroidal Wave Functions (PSWFs) or more commonly as the (classical) Slepian functions on the real line. Owing to their many interesting properties [5], the Slepian functions have found a wide variety of applications in several diverse fields of science and engineering such as information and communication theory [6], [7], signal detection and estimation [8], signal interpolation and extrapolation [9], [10], compressed sensing [11], signal recovery and reconstruction [12]–[14], sampling theory [15]–[17], neuroscience [18], [19], optics [20], and many more.

The wide applicability of the one-dimensional time-domain Slepian functions motivated researchers to extend this concept to higher dimensions. The authors in [1] laid the foundation for the extension of the concentration problem to the two-dimensional case in the Cartesian plane [3] where the spatial region in the form of circular disks has been considered. Later, the planar Slepian functions for other geometries and arbitrary regions in general were also explored in [21]. However, even these developments seemed insufficient for some applications. For instance, in planetary sciences, the use of the two-dimensional planar Slepian functions based on the local flat approximation was prohibited due to the inherent curved surface of a planet. To support such applications and beyond, the spherical analogue for the one-dimensional Slepian concentration problem was proposed in [22], [23], herein referred to as the (classical) Slepian concentration problem on the sphere. Since then, the Slepian functions on the sphere have been utilized for applications in geophysics [24], [25], cosmology [26], geodesy [27], acoustics [28], [29], planetary sciences [23], signal estimation [30], [31], spectral analysis [32], hydrology [33], graph theory [34]–[37], etc.

For many years a great effort has been devoted to the study of the Slepian concentration problem on the sphere and its applications. In this context, the development of algorithms for the efficient computation of the Slepian functions has been widely investigated [23], [24], [27], [38]. For estimating the potential fields of a planet, the spherical Slepian functions provide a more practical solution as compared to the commonly used damped least-squares spherical harmonic approach [27]. The spherical Slepian functions also find applications in geophysics, e.g., in the decomposition of lithospheric magnetic field models [25].

Apart from potential field estimation in geodesy, an important problem arises in cosmology: the estimation of the spectrum of the cosmic microwave background (CMB) radiation. To address this problem several works have appeared

The video presentation of the paper is available at https://youtu.be/PY42h2naqrk.

W. Nafees and Z. Khalid are with School of Science and Engineering, Lahore University of Management Sciences, Lahore, Pakistan. Rodney A. Kennedy is with the Research School of Engineering, College of Engineering and Computer Science, The Australian National University, Canberra, Australia.

W. Nafees is supported by HEC NRPU Project no. 5925. R. A. Kennedy is supported by the Australian Research Council's Discovery Projects funding scheme (Project no. DP170101897).

E-mail: wajeeha.nafees@lums.edu.pk, zubair.khalid@lums.edu.pk, rodney.kennedy@anu.edu.au

This article has been accepted for publication in a future issue of this journal, but has not been fully edited. Content may change prior to final publication. Citation information: DOI 10.1109/TSP.2020.2983644, IEEE Transactions on Signal Processing

in the recent years documenting the spectral analysis on the sphere that utilizes the Slepian functions [39], [40]. These studies indicate that the spectral analysis and estimation have gained fundamental importance for explaining the behaviour of random processes on spherical bodies. However, in some settings one does not have access to, or may simply not be interested in, the values of the function outside some particular region of the sphere (e.g., due to noise contamination). In such cases it is convenient to use the spatially limited data for signal analysis on the sphere [41]. In [26], the authors use Slepian functions to estimate the spectrum of a noisy, isotropic process in a bounded region on the sphere. The Slepian functions have also been used as localization windows for energy spectrum estimation [24], [30], [32].

In a recent work, the Slepian functions have been utilized for the reconstruction of the head-related transfer function (HRTF) on the sphere, where it has been demonstrated that the proposed reconstruction technique allows more accurate results as compared to the methods based on using the conventional spherical harmonic basis functions [29]. Since the Slepian functions optimally reduce the estimation bias and leakage effects as compared to other methods, thery have been used for deriving estimates of water storage variations in different regions of the Earth using data collected by satellites [33].

In this work, we introduce weighting functions in the formulation of the classical Slepian concentration problem on the sphere. We assign different values to the weighting functions in the proposed generalized formulation to present two variants, differential and weighted, of the concentration problem on the sphere for finding band-limited functions with optimal energy concentration in the spatial domain. In the first variant, we consider two spatial regions on the sphere and determine band-limited functions on the sphere such that the difference in the energy concentration of the function over the regions is maximized. Such maximization enables enhancement of the energy over one region at the cost of it in the other region. We note that the differential Slepian problem was first introduced in [14] for one-dimensional (time-domain) signals. In the second variant, we use non-negative weighting as a window function in the formulation of the Slepian problem to optimally concentrate the signal energy in the spatial domain. We formulate each of the problems in the harmonic domain as an eigenvalue problem and review the properties of the eigenfunctions, referred to as Slepian functions, which serve as an alternative basis for the representation of band-limited signals on the sphere. We also demonstrate the use of Slepian functions for localized energy spectrum estimation and robust modeling of the signal on the sphere.

We present our contributions by organizing the remainder of the paper as follows. We review the mathematical background in Section II and present the differential and the weighted Slepian problems on the sphere in Section III, where we also derive the properties of the proposed Slepian functions and provide an illustration. The use of Slepian functions for spectrum estimation and robust modeling is demonstrated in Section IV before making the concluding remarks in Section V.

II. Mathematical Preliminaries

A. Signals on the Sphere

A unit sphere or 2-sphere, denoted by $\mathbb{S}^2$, is defined as $\mathbb{S}^2 \triangleq \{\widehat{\boldsymbol{u}} \in \mathbb{R}^3 : \|\widehat{\boldsymbol{u}}\|_2 = 1\}$, where $\|\cdot\|_2$ is the Euclidean norm and $\widehat{\boldsymbol{u}}$ denotes a vector in 3D Euclidean domain. In the spherical coordinates system, a point on the unit sphere is described using two parameters, namely the co-latitude $\theta \in [0, \pi]$ and longitude $\phi \in [0, 2\pi)$, and mathematically written as $\widehat{\boldsymbol{u}} \equiv \widehat{\boldsymbol{u}}(\theta, \phi) \triangleq (\sin\theta\cos\phi, \sin\theta\sin\phi, \cos\theta) \in \mathbb{S}^2$. We consider complex-valued, square-integrable functions $f(\widehat{\boldsymbol{u}}) \equiv f(\theta, \phi)$ on the unit sphere, which form a complete Hilbert space, denoted by $L^2(\mathbb{S}^2)$. For any two functions f_1, f_2 defined on the unit sphere $\mathbb{S}^2$ the inner product associated with $L^2(\mathbb{S}^2)$ is

$$\langle f_1, f_2\rangle \triangleq \int_{\mathbb{S}^2} f_1(\widehat{\boldsymbol{u}})\overline{f_2(\widehat{\boldsymbol{u}})}\, ds(\widehat{\boldsymbol{u}}), \tag{1}$$

where $ds(\widehat{\boldsymbol{u}}) \triangleq \sin\theta\, d\theta d\phi$, $\overline{(\cdot)}$ denotes the complex conjugate operation and the integration $\int_{\mathbb{S}^2} = \int_{\theta=0}^{\pi}\int_{\phi=0}^{2\pi}$ is over the whole sphere. The inner product in (1) induces a norm $\|f\| \triangleq \langle f, f\rangle^{1/2}$. We refer to the functions with finite energy (or induced norm) as "signals on the sphere".

B. Spherical Harmonics

The spherical harmonic functions (or spherical harmonics) form a set of complete basis functions for the Hilbert space $L^2(\mathbb{S}^2)$ and are defined as

$$Y_\ell^m(\widehat{\boldsymbol{u}}) \triangleq \sqrt{\frac{2\ell+1}{4\pi}\frac{(\ell-m)!}{(\ell+m)!}}\, P_\ell^m(\cos\theta)\, e^{im\phi} \tag{2}$$

where $0 \le \ell \le \infty$ is the angular degree, $-\ell \le m \le \ell$ is the angular order and $P_\ell^m(\mu)$ denotes the associate Legendre polynomial of degree ℓ and order m. With the adopted definition, the spherical harmonics are orthonormal, i.e.,

$$\int_{\mathbb{S}^2} Y_\ell^m(\widehat{\boldsymbol{u}})\overline{Y_{\ell'}^{m'}(\widehat{\boldsymbol{u}})} ds(\widehat{\boldsymbol{u}}) = \delta_{\ell\ell'}\delta_{mm'}, \tag{3}$$

where $\delta_{\ell\ell'}$ represents the Kronecker delta. Due to the completeness of the spherical harmonic basis functions, any signal $f \in L^2(\mathbb{S}^2)$ can be expanded as

$$f(\widehat{\boldsymbol{u}}) = \sum_{\ell=0}^{\infty}\sum_{m=-\ell}^{\ell} (f)_\ell^m Y_\ell^m(\widehat{\boldsymbol{u}}), \tag{4}$$

where

$$(f)_\ell^m \triangleq \langle f, Y_\ell^m\rangle = \int_{\mathbb{S}^2} f(\widehat{\boldsymbol{u}})\overline{Y_\ell^m(\widehat{\boldsymbol{u}})}\, ds(\widehat{\boldsymbol{u}}), \tag{5}$$

represents the spherical harmonic coefficient of degree ℓ and order m. We adopt $\sum_{\ell m}^{\infty} \equiv \sum_{\ell=0}^{\infty}\sum_{m=-\ell}^{\ell}$ for succinct representation in the sequel. The spherical harmonic coefficients represent the signal f in the harmonic (spectral) domain. The equations (5) and (4) are referred to as the spherical harmonic transform (SHT) and the inverse SHT respectively.

C. Space-limited and Band-limited Functions

A signal $f \in L^2(\mathbb{S}^2)$ is said to be space-limited within the spatial region $R \subset \mathbb{S}^2$ if it has the form

$$f(\widehat{\boldsymbol{u}}) = \begin{cases} f(\widehat{\boldsymbol{u}}), & \widehat{\boldsymbol{u}} \in R, \\ 0, & \text{otherwise.} \end{cases} \tag{6}$$

This article has been accepted for publication in a future issue of this journal, but has not been fully edited. Content may change prior to final publication. Citation information: DOI 10.1109/TSP.2020.2983644, IEEE Transactions on Signal Processing

A signal $f \in L^2(\mathbb{S}^2)$ is said to be band-limited at L if $(f)_\ell^m = 0,\ \forall \ell \geq L$, and can be expanded using the spherical harmonic functions as

$$f(\widehat{\boldsymbol{u}}) = \sum_{\ell m=0}^{L-1} (f)_\ell^m Y_\ell^m(\widehat{\boldsymbol{u}}), \tag{7}$$

These band-limited signals form a subspace, denoted by $\mathcal{H}_L$, of dimension L^2. We use the vector notation $\boldsymbol{f}$ to represent a column vector of length L^2 containing the spherical harmonic coefficients such that

$$\boldsymbol{f} \triangleq [\dots f_n \dots] = [(f)_0^0, (f)_1^{-1}, (f)_1^0, (f)_1^1, \dots, (f)_{L-1}^{L-1}]^T \in \mathbb{C}^{L^2} \tag{8}$$

where the index $n = \ell^2 + \ell + m + 1$ takes the values $n = 1, 2, \dots, L^2$. The spatial and spectral representations of the signal are related through isomorphism [42]

$$\langle f_1, f_2 \rangle = \langle \boldsymbol{f}_1, \boldsymbol{f}_2 \rangle_{\mathbb{C}} \triangleq \boldsymbol{f}_2^H \boldsymbol{f}_1, \tag{9}$$

where $(\cdot)^H$ denotes the Hermitian operation.

D. Energy Spectrum

Using Parseval's theorem, we can find the total energy[1] of a function $f \in L^2(\mathbb{S}^2)$ on the sphere in terms of its spherical harmonic coefficients as [32]

$$\|f\|^2 = \int_{\mathbb{S}^2} |f(\widehat{\boldsymbol{u}})|^2 ds(\widehat{\boldsymbol{u}}) = \sum_{\ell=0}^{\infty} S_{ff}(\ell), \tag{10}$$

where S_{ff} is the energy per degree defined as

$$S_{ff}(\ell) = \sum_{m=-\ell}^{\ell} (f)_\ell^m \overline{(f)_\ell^m}. \tag{11}$$

The cross-energy spectrum of two functions $f_1, f_2 \in L^2(\mathbb{S}^2)$ is

$$\int_{\mathbb{S}^2} f_1(\widehat{\boldsymbol{u}}) \overline{f_2(\widehat{\boldsymbol{u}})} ds(\widehat{\boldsymbol{u}}) = \sum_{\ell=0}^{\infty} S_{f_1 f_2}(\ell), \tag{12}$$

where $S_{f_1 f_2}$ is the cross-energy per degree defined as

$$S_{f_1 f_2}(\ell) = \sum_{m=-\ell}^{\ell} (f_1)_\ell^m \overline{(f_2)_\ell^m}. \tag{13}$$

III. Differential and Weighted Slepian Concentration Problems on the Sphere

The Slepian concentration problem has been formulated and analysed for signals defined on the one-dimensional time domain, the two-dimensional Cartesian plane and the higher dimensions (in the Euclidean setting). In [23] and [43], the Slepian concentration problem has been formulated for signals defined on the unit sphere and the unit ball respectively. In this section, we revisit the Slepian concentration problem for signals on the unit sphere and present a generalized framework and the variations of the concentration problem. We define the generalization of the Slepian concentration problem of finding band-limited function $f \in \mathcal{H}_L$ as

$$\lambda = \max_{f \in \mathcal{H}_L} \left(\frac{\displaystyle\int_{\mathbb{S}^2} h(\widehat{\boldsymbol{u}}) |f(\widehat{\boldsymbol{u}})|^2 ds(\widehat{\boldsymbol{u}})}{\displaystyle\int_{\mathbb{S}^2} g(\widehat{\boldsymbol{u}}) |f(\widehat{\boldsymbol{u}})|^2 ds(\widehat{\boldsymbol{u}})} \right), \tag{14}$$

[1]The total energy is 4π times the total power for signals on the sphere.

where $h(\widehat{\boldsymbol{u}})$ and $g(\widehat{\boldsymbol{u}})$ represent the weighting functions and λ is the ratio of the weighted energies of the function. We note that the different choices of the weighting functions $h(\widehat{\boldsymbol{u}})$ and $g(\widehat{\boldsymbol{u}})$ in (14) lead to different variations of the Slepian problem on the sphere. Using (7), the spectral domain formulation for (14) is given by

$$\lambda = \frac{\displaystyle\sum_{\ell m}^{L-1} (f)_\ell^m \sum_{\ell' m'}^{L-1} H_{\ell\ell'}^{mm'} \overline{(f)_{\ell'}^{m'}}}{\displaystyle\sum_{\ell m}^{L-1} (f)_\ell^m \sum_{\ell' m'}^{L-1} G_{\ell\ell'}^{mm'} \overline{(f)_{\ell'}^{m'}}}, \tag{15}$$

where

$$H_{\ell\ell'}^{mm'} \triangleq \int_{\mathbb{S}^2} h(\widehat{\boldsymbol{u}}) Y_\ell^m(\widehat{\boldsymbol{u}}) \overline{Y_{\ell'}^{m'}(\widehat{\boldsymbol{u}})} ds(\widehat{\boldsymbol{u}}) \tag{16}$$

$$G_{\ell\ell'}^{mm'} \triangleq \int_{\mathbb{S}^2} g(\widehat{\boldsymbol{u}}) Y_\ell^m(\widehat{\boldsymbol{u}}) \overline{Y_{\ell'}^{m'}(\widehat{\boldsymbol{u}})} ds(\widehat{\boldsymbol{u}}). \tag{17}$$

By defining the coupling matrices $\boldsymbol{H}$ and $\boldsymbol{G}$ with elements $H_{\ell\ell'}^{mm'}$ and $G_{\ell\ell'}^{mm'}$ respectively and adopting the same indexing of these matrices as adopted for indexing the spherical harmonic coefficients in a vector $\boldsymbol{f}$ in (8), we can rewrite (15) in the matrix form as

$$\lambda = \max_{\boldsymbol{f}} \left(\frac{\boldsymbol{f}^H \boldsymbol{H} \boldsymbol{f}}{\boldsymbol{f}^H \boldsymbol{G} \boldsymbol{f}} \right). \tag{18}$$

A. Classical Slepian Concentration Problem on the Sphere

For the classical Slepian problem on the sphere [22], [23], we have the following weighting functions in the spatial domain:

$$h(\widehat{\boldsymbol{u}}) = I_R(\widehat{\boldsymbol{u}}), \qquad g(\widehat{\boldsymbol{u}}) = 1, \tag{19}$$

where $I_R(\widehat{\boldsymbol{u}})$ represents the indicator function of the region R defined as

$$I_R(\widehat{\boldsymbol{u}}) \triangleq \begin{cases} 1 & \widehat{\boldsymbol{u}} \in R, \\ 0 & \widehat{\boldsymbol{u}} \in \mathbb{S}^2 \backslash R. \end{cases} \tag{20}$$

Here $R \subset \mathbb{S}^2$ represents a region that may be a single connected region or a union of disjoint sub-regions such that $R = R_a \cup R_b \cup \dots$. The area of the region R is given by $|R| = \int_R ds(\widehat{\boldsymbol{u}})$. The solution of the classical Slepian problem yields a family of L^2 eigenfunctions referred to as the classical Slepian functions. These eigenfunctions are mutually orthogonal over the regions R and $\mathbb{S}^2\backslash R$ and orthonormal over the unit sphere. Due to the optimal localization and the orthogonality of the classical Slepian functions over the region R, these have been used in applications which include, but are not limited to, spectral analysis, signal estimation, signal interpolation and extrapolation and polar gap problem in geodesy and cosmology [23], [26], [27].

B. Differential Slepian Concentration Problem on the Sphere

Here we present a variation of the Slepian problem by considering two disjoint regions on the sphere. We counter-balance the energy concentration between the two regions such that the energy concentration in one region is enhanced at the expense of diminishing energy concentration in the other. Let R_1 and R_2 be the two regions, such that $R_1 \cap R_2 = \emptyset$,

This article has been accepted for publication in a future issue of this journal, but has not been fully edited. Content may change prior to final publication. Citation information: DOI 10.1109/TSP.2020.2983644, IEEE Transactions on Signal Processing

where the energy concentration is required to be maximized and minimized respectively at the same time. For this variant of the Slepian concentration problem, the weighting functions are defined to be

$$\begin{aligned} h(\widehat{\boldsymbol{u}}) &= I_{R_1}(\widehat{\boldsymbol{u}}) - I_{R_2}(\widehat{\boldsymbol{u}}), \\ g(\widehat{\boldsymbol{u}}) &= 1, \end{aligned} \tag{21}$$

where $I_{R_1}(\widehat{\boldsymbol{u}})$ and $I_{R_2}(\widehat{\boldsymbol{u}})$ represent the indicator functions for the regions R_1 and R_2 respectively.

By defining the inner product over the region R_k as

$$\langle f_1, f_2 \rangle_{R_k} \triangleq \int_{R_k} f_1(\widehat{\boldsymbol{u}}) \overline{f_2(\widehat{\boldsymbol{u}})}\, ds(\widehat{\boldsymbol{u}}), \tag{22}$$

that quantifies the cross-energy spectrum of two functions f_1, f_2 over the region R_k, the numerator in (14), for the choice of weighting functions given in (21), takes the following form

$$\int_{\mathbb{S}^2} h(\widehat{\boldsymbol{u}}) |f(\widehat{\boldsymbol{u}})|^2 ds(\widehat{\boldsymbol{u}}) = \langle f, f \rangle_{R_1} - \langle f, f \rangle_{R_2}. \tag{23}$$

Due to the fact that (23) represents the difference of energy of the function over the two regions, we refer to this variant of the concentration problem as the differential Slepian problem. It is trivial to show that the problem in (23) reduces to the classical Slepian problem if $R_2 = \emptyset$. Analogous to (18), the differential Slepian concentration problem can be written in spectral domain form as the Rayleigh quotient

$$\lambda = \max_{\boldsymbol{f}} \left(\frac{\boldsymbol{f}^H \boldsymbol{H} \boldsymbol{f}}{\boldsymbol{f}^H \boldsymbol{f}} \right), \tag{24}$$

where

$$\boldsymbol{H} = {}_1\boldsymbol{D} - {}_2\boldsymbol{D}, \quad \boldsymbol{G} = \boldsymbol{I}, \tag{25}$$

$${}_k\boldsymbol{D} = \begin{bmatrix} {}_kD_{00}^{00} & \cdots & {}_kD_{00}^{L-1\,L-1} \\ \cdots & \ddots & \cdots \\ {}_kD_{L-1\,L-1}^{00} & \cdots & {}_kD_{L-1\,L-1}^{L-1\,L-1} \end{bmatrix}, \; k = 1, 2, \tag{26}$$

with ${}_kD_{\ell\ell'}^{mm'} = \int_{R_k} Y_\ell^m(\widehat{\boldsymbol{u}}) \overline{Y_{\ell'}^{m'}(\widehat{\boldsymbol{u}})} ds(\widehat{\boldsymbol{u}})$ for $k = 1, 2$. The solution $\boldsymbol{f}$ that maximizes λ in (24) is also a solution of the eigenvalue problem

$$\boldsymbol{H}\boldsymbol{f} = \lambda \boldsymbol{f}. \tag{27}$$

Since $\boldsymbol{H}$ is Hermitian matrix, the solution of the eigenvalue problem, (27), yields a set of L^2 real eigenvalues $\{\lambda_\alpha\}$ and L^2 orthogonal eigenvectors $\{\boldsymbol{f}_\alpha\}$ for $\alpha = 1, 2, \ldots, L^2$ which we choose to be orthonormal such that

$$\begin{aligned} \langle \boldsymbol{f}_\alpha, \boldsymbol{f}_\beta \rangle_{\mathbb{C}} &= \delta_{\alpha\beta}, \quad \alpha, \beta = 1, 2, \ldots, L^2, \\ \langle \boldsymbol{f}_\alpha, \boldsymbol{H}\boldsymbol{f}_\beta \rangle_{\mathbb{C}} &= \lambda_\alpha \delta_{\alpha\beta}, \quad \alpha, \beta = 1, 2, \ldots, L^2. \end{aligned} \tag{28}$$

The choice of the weighting function $h(\widehat{\boldsymbol{u}})$ in (21) implies that $|\lambda_\alpha| \le 1$. We index the eigenvalues and the associated eigenvectors in the non-increasing order such that $1 \ge \lambda_1 \ge \lambda_2 \ldots \lambda_{L^2} \ge -1$. Using (16), we express (27) as

$$\sum_{\ell' m'}^{L-1} \int_{\mathbb{S}^2} h(\widehat{\boldsymbol{u}}) Y_\ell^m(\widehat{\boldsymbol{u}}) \overline{Y_{\ell'}^{m'}(\widehat{\boldsymbol{u}})} ds(\widehat{\boldsymbol{u}}) (f)_{\ell'}^{m'} = \lambda (f)_\ell^m, \tag{29}$$

By multiplying (29) with $Y_\ell^m(\widehat{\boldsymbol{v}})$ followed by the summation over $0 \le \ell' < L$ and $|m'| \le \ell'$, we obtain the formulation of an equivalent eigenvalue problem in the spatial domain represented by the Fredholm equation given by

$$\int_{\mathbb{S}^2} D(\widehat{\boldsymbol{u}}, \widehat{\boldsymbol{v}}) f(\widehat{\boldsymbol{v}}) ds(\widehat{\boldsymbol{v}}) = \lambda f(\widehat{\boldsymbol{u}}), \tag{30}$$

where

$$D(\widehat{\boldsymbol{u}}, \widehat{\boldsymbol{v}}) = \left(\sum_{\ell m}^{L-1} Y_\ell^m(\widehat{\boldsymbol{u}}) Y_\ell^m(\widehat{\boldsymbol{v}}) \right) (I_{R_1}(\widehat{\boldsymbol{u}}) - I_{R_2}(\widehat{\boldsymbol{u}})). \tag{31}$$

Each eigenvector $\boldsymbol{f}_\alpha$ presents the spectral domain representation of the eigenfunction $f_\alpha \in \mathcal{H}_L$. The spatial domain eigenfunction $f_\alpha(\widehat{\boldsymbol{u}})$, related to the eigenvector $\boldsymbol{f}_\alpha$ through $\langle f_\alpha, Y_\ell^m \rangle = (f_\alpha)_\ell^m$, for $\alpha = 1, 2, \ldots, L^2$ is referred to as the differential Slepian function. The eigenvalue λ_α quantifies the difference in the energy concentration of the eigenfunction f_α over the regions R_1 and R_2. The differential Slepian function $f_1(\widehat{\boldsymbol{u}})$, associated with the largest eigenvalue, is the function with maximum energy concentration in the region R_1. Similarly, the differential Slepian function $f_{L^2}(\widehat{\boldsymbol{u}})$, associated with the lowest eigenvalue, is the function with maximum energy concentration in the region R_2.

C. Properties of Differential Slepian Functions

Property 1: Orthogonality of the Differential Slepian Functions: The differential Slepian functions are orthonormal over $\mathbb{S}^2$, i.e.,

$$\langle f_\alpha, f_\beta \rangle_{\mathbb{S}^2} = \delta_{\alpha\beta}, \tag{32}$$

which simply follows from the orthonormality of the spherical harmonics and (28). The differential Slepian functions are orthogonal over the regions R_1 and R_2 such that,

$$\langle f_\alpha, f_\beta \rangle_{R_1} - \langle f_\alpha, f_\beta \rangle_{R_2} = \lambda_\alpha \, \delta_{\alpha\beta}, \tag{33}$$

which can be shown using (28). Furthermore, the differential Slepian functions are nearly orthogonal over R_1, that is,

$$\begin{aligned} \alpha = \beta : &\quad \langle f_\alpha, f_\alpha \rangle_{R_1} \ge \lambda_\alpha \\ \alpha \ne \beta : &\quad |\langle f_\alpha, f_\beta \rangle_{R_1}| \le \frac{\sqrt{(1-\lambda_\alpha)(1-\lambda_\beta)}}{2}. \end{aligned} \tag{34}$$

Similar results hold true for the region R_2:

$$\begin{aligned} \alpha = \beta : &\quad \langle f_\alpha, f_\alpha \rangle_{R_2} \ge -\lambda_\alpha \\ \alpha \ne \beta : &\quad |\langle f_\alpha, f_\beta \rangle_{R_2}| \le \frac{\sqrt{(1+\lambda_\alpha)(1+\lambda_\beta)}}{2}. \end{aligned} \tag{35}$$

For $\alpha \ne \beta$ the cosine of the angle between any two differential Slepian functions is defined as

$$|\cos\gamma_{f_\alpha, f_\beta}| \triangleq \frac{\langle f_\alpha, f_\beta \rangle}{|f_\alpha|\,|f_\beta|}, \tag{36}$$

and can be computed as

$$|\cos\gamma_{f_\alpha, f_\beta}| \le \frac{1}{2} \frac{\sqrt{(1-\lambda_\alpha)(1-\lambda_\beta)}}{\lambda_\alpha \lambda_\beta}, \quad \lambda_\alpha, \lambda_\beta > 0, \tag{37}$$

$$|\cos\gamma_{f_\alpha, f_\beta}| \le \frac{1}{2} \frac{\sqrt{(1+\lambda_\alpha)(1+\lambda_\beta)}}{\lambda_\alpha \lambda_\beta} \quad \lambda_\alpha, \lambda_\beta < 0. \tag{38}$$

We provide the derivation of these relationships in Appendix A.

Property 2: Completeness of the Differential Slepian Functions: The differential Slepian functions form a complete basis for the space $\mathcal{H}_L$. This follows from the orthonormality of the differential Slepian functions and the dimensionality of $\mathcal{H}_L$.

Property 3: Spectrum of Eigenvalues: Despite the matrix $\boldsymbol{H}$ being indefinite, the eigenvalues are real and lie in $[-1, +1]$ due to the normalization adopted in (24). The eigenvalues

This article has been accepted for publication in a future issue of this journal, but has not been fully edited. Content may change prior to final publication. Citation information: DOI 10.1109/TSP.2020.2983644, IEEE Transactions on Signal Processing

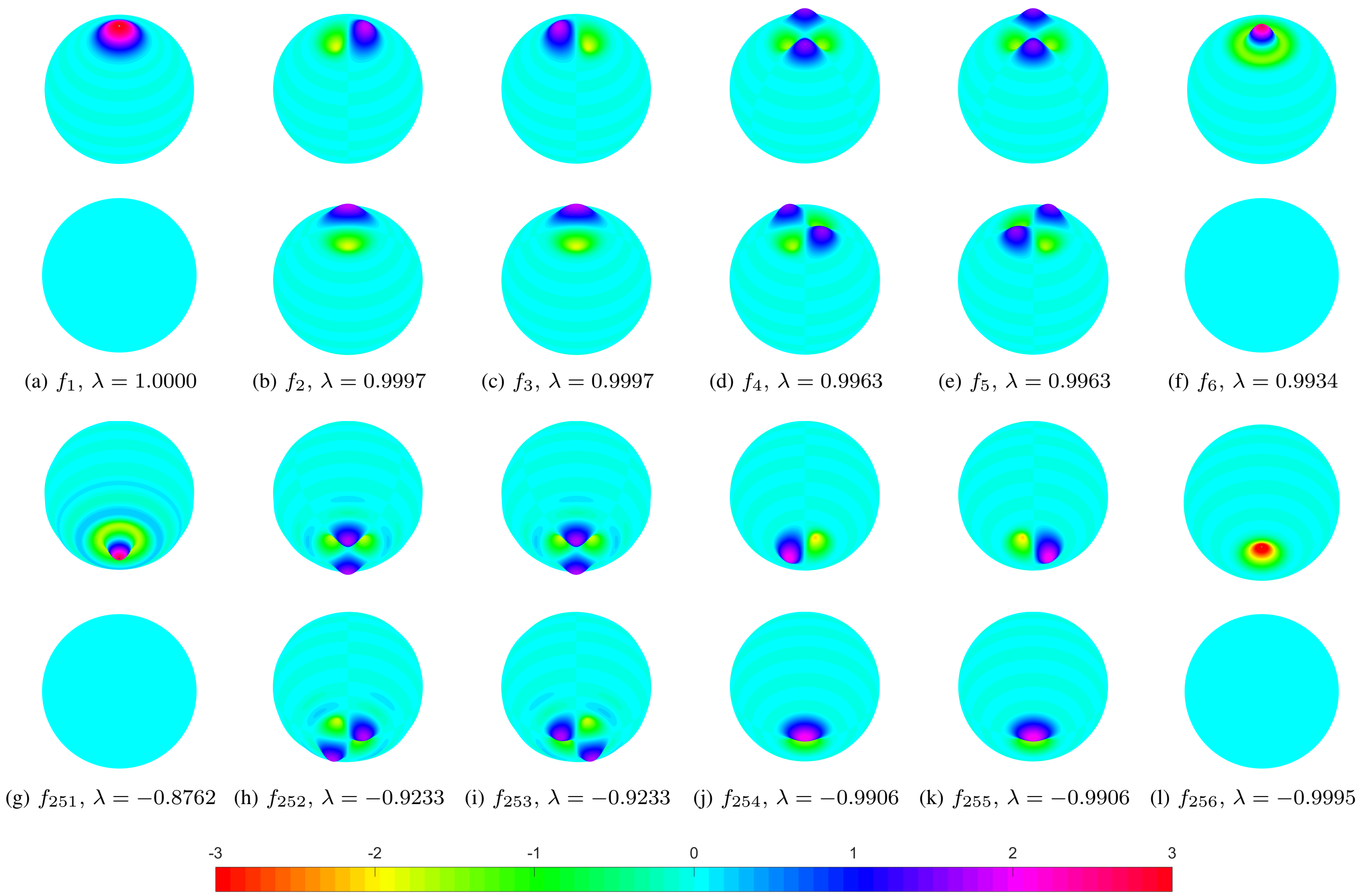

Fig. 1: Slepian functions in the spatial domain obtained as a solution of differential concentration problem for regions $R_1 = \{\widehat{\boldsymbol{u}}(\theta,\phi) \in \mathbb{S}^2 | \theta \leq \pi/6\}$, $R_2 = \{\widehat{\boldsymbol{u}}(\theta,\phi) \in \mathbb{S}^2 | \theta \geq 7\pi/8\}$ and band-limit $L = 16$. For each subplot, the top and bottom plots represent the real and imaginary part of the Slepian function respectively. The first six Slepian functions are optimally concentrated in the region R_1 and are plotted in (a)-(f) with eigenvalues indicated and view set at azimuth of 0 and elevation of $\pi/4$. The last six Slepian functions are optimally concentrated in the region R_2 and are plotted in (g)-(l) with eigenvalues indicated and view set at azimuth of 0 and elevation of $3\pi/4$.

closer to $+1$ (or -1) represent optimal (maximal) energy concentration in the region R_1 (or R_2). The sum of eigenvalues of the differential Slepian problem is given by

$$\begin{aligned} N_H &= \sum_{\alpha=1}^{L^2} \lambda_\alpha = \text{trace}({}_1\boldsymbol{D}) - \text{trace}({}_2\boldsymbol{D}) \qquad (39)\\ &= \sum_{\ell m}^{L} ({}_1D_{\ell\ell}^{mm} - {}_2D_{\ell\ell}^{mm}) = \int_{\mathbb{S}^2} D(\widehat{\boldsymbol{u}},\widehat{\boldsymbol{u}}) ds(\widehat{\boldsymbol{u}})\\ &= \int_{\mathbb{S}^2} \sum_{\ell=0}^{L-1} \frac{2\ell+1}{4\pi} P_\ell^0(\widehat{\boldsymbol{u}}\cdot\widehat{\boldsymbol{u}}) \left(I_{R_1}(\widehat{\boldsymbol{u}}) - I_{R_2}(\widehat{\boldsymbol{u}})\right) ds(\widehat{\boldsymbol{u}})\\ &= \sum_{\ell=0}^{L-1} \frac{2\ell+1}{4\pi} \left(\int_{R_1} ds(\widehat{\boldsymbol{u}}) - \int_{R_2} ds(\widehat{\boldsymbol{u}}) \right)\\ &= \frac{L^2}{4\pi}(|R_1| - |R_2|), \end{aligned}$$

where $|R_k|, k = 1,2$ represents the area of the k-th region and we have employed the spherical harmonic addition theorem [42]. To find the number of optimally concentrated eigenfunctions in the region R_k, the Shannon number (the sum of the eigenvalues of the classical Slepian problem solved for the k-th region, denoted by N_k) seems to be a good estimate. It is easy to show that $N_H = N_1 - N_2$. For the differential Slepian problem, it can be shown that the difference between the Shannon number, say N_1, obtained when the classical Slepian problem is applied to region R_1 and the sum of positive eigenvalues of the differential problem is equal to the sum of the Shannon number, say N_2, obtained when the classical Slepian problem is applied to region R_2 and the sum of negative eigenvalues of the differential problem. This can be expressed mathematically as

$$N_1 - \sum_\alpha \lambda_\alpha^+ = N_2 + \sum_\alpha \lambda_\alpha^-, \qquad (40)$$

where λ_α^+ and λ_α^- represent the positive and negative eigenvalues of the differential Slepian problem respectively.

Property 4: Symmetrical Solutions: Since ${}_1\boldsymbol{D} - {}_2\boldsymbol{D} = -({}_2\boldsymbol{D} - {}_1\boldsymbol{D})$, the solution to the original problem in (23) holds, with just an inversion in the signs of the eigenvalues λ_α, that is, if we switch the role of R_1 and R_2 as the regions where we require enhanced and diminished energy concentration respectively.

This article has been accepted for publication in a future issue of this journal, but has not been fully edited. Content may change prior to final publication. Citation information: DOI 10.1109/TSP.2020.2983644, IEEE Transactions on Signal Processing

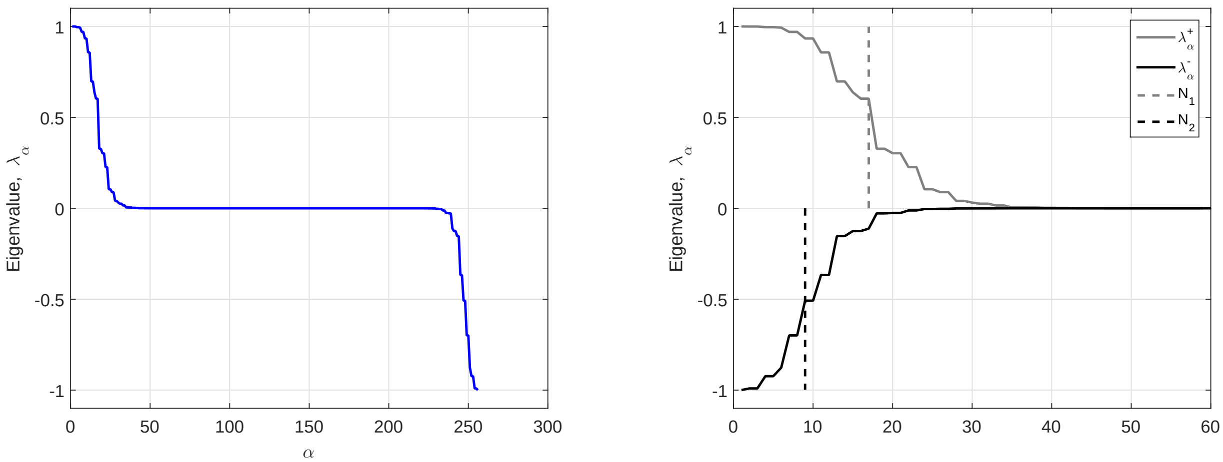

(a) Spectrum of Eigenvalues

(b) Positive and negative eigenvalues spectra

Fig. 2: Spectrum of eigenvalues obtained when the differential Slepian concentration problem is solved using (24) for $L = 16$. (a) The consolidated spectrum of eigenvalues, showing the two transitions associated with the two regions. (b) The positive and negative eigenvalue spectra. The dashed lines show the Shannon numbers $N_1 = 16$ and $N_2 = 9$ respectively for the two regions.

D. Illustration

For the differential Slepian concentration problem, we provide an illustration and analyse the eigenfunctions, spectrum of eigenvalues, orthogonality properties and energy enhancement enabled by the eigenfunctions over the regions of interest. We solve the differential concentration problem for R_1 taken as North polar cap of co-latitudinal radius $\theta_1 = \pi/6$, that is, $R_1 = \{\widehat{\boldsymbol{u}}(\theta, \phi) \in \mathbb{S}^2 | \, \theta \leq \pi/6\}$, R_2 as South polar cap of co-latitudinal radius $\theta_2 = \pi/8$, that is, $R_2 = \{\widehat{\boldsymbol{u}}(\theta, \phi) \in \mathbb{S}^2 | \, \theta \geq 7\pi/8\}$ and band-limit $L = 16$. Fig. 1 shows the real and imaginary parts of the first 6 eigenfunctions, $f_1, f_2, \dots, f_6$ and the last 6 eigenfunctions, $f_{251}, f_{252}, \dots, f_{256}$, where it is evident that the last 6 eigenfunctions are mostly concentrated in the region R_2 (Property 3).

We also analyse the spectrum of eigenvalues in Fig. 2, where the two phase transitions visible in Fig. 2 (a) are associated with the two regions. We also plot the positive and negative eigenvalues spectra in Fig. 2 (b). The dashed lines show the Shannon number N_1 and N_2 associated with the eigenfunctions obtained from the solution of the classical Slepian problem on regions R_1 and R_2 respectively.

To analyse the mutual orthogonality of the eigenfunctions over the spatial regions of interest, we compute the inner product of the eigenfunctions as well as the bounds on the inner product given in (34) and (35). The actual inner products are plotted in Fig. 3 (a) and (b) that are consistent with the bounds plotted in Fig. 3 (c) and (d).

The differential Slepian problem gives eigenfunctions which have increased energy in the region R_1 while the energy in the region R_2 decreases. We compare the energies of the classical Slepian functions constructed for region R_1 and differential Slepian functions and illustrate the reduction of energy in the region R_2 in Fig. 4, where E_{class} is the energy of the classical Slepian functions in the region R_2 and the energy E_{diff} refers to the energy of the differential Slepian functions in the region R_2. It can be seen in the figure that E_{diff} is less than E_{class} thus validating the claim made in the prequel.

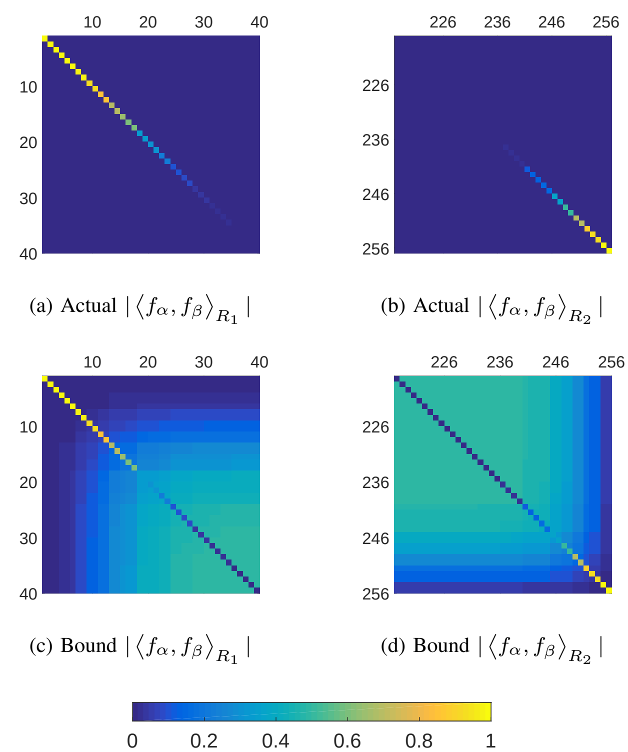

(a) Actual $|\langle f_\alpha, f_\beta \rangle_{R_1}|$

(b) Actual $|\langle f_\alpha, f_\beta \rangle_{R_2}|$

(c) Bound $|\langle f_\alpha, f_\beta \rangle_{R_1}|$

(d) Bound $|\langle f_\alpha, f_\beta \rangle_{R_2}|$

Fig. 3: Actual inner product of eigenfunctions on region R_1 and R_2 in the top row and their bounds in the bottom row respectively.

E. Rotationally Symmetric Antipodal Regions

The regions R_1 and R_2 associated with the differential Slepian problem can have any arbitrary orientation on the sphere. If the two regions are oriented as shown in

This article has been accepted for publication in a future issue of this journal, but has not been fully edited. Content may change prior to final publication. Citation information: DOI 10.1109/TSP.2020.2983644, IEEE Transactions on Signal Processing

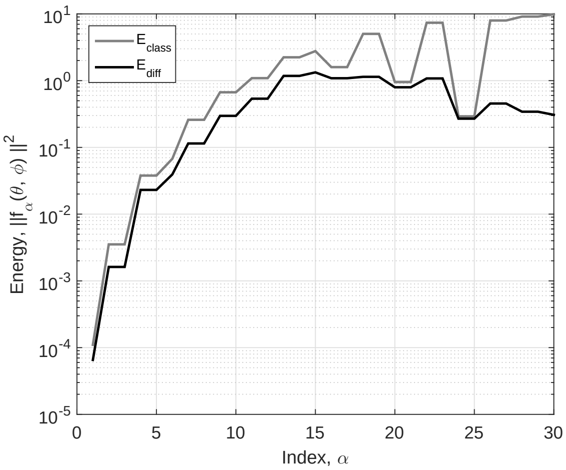

Fig. 4: E_{class} and E_{diff} represent the energy of the region R_2 calculated using the classical and differential Slepian approach respectively.

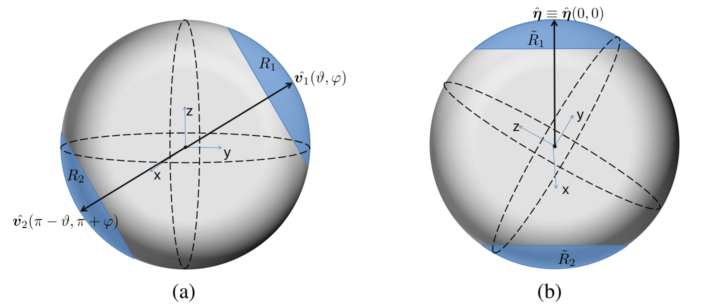

Fig. 5: The blue part of the sphere shows the regions of interest. (a) Rotationally symmetric antipodal regions R_1 and R_2, (b) Azimuthally symmetric antipodal regions $\tilde{R}_1$ and $\tilde{R}_2$ obtained by rotating the sphere in (a) by $\pi - \varphi$ around z-axis and then by ϑ around y-axis.

Fig. 5(a), they are categorized as rotationally symmetric around $\widehat{\boldsymbol{v}}_1(\vartheta,\varphi) \in \mathbb{S}^2$ (or $\widehat{\boldsymbol{v}}_2(\pi-\vartheta,\pi+\varphi) \in \mathbb{S}^2$) and antipodal regions (since $\widehat{\boldsymbol{v}}_1$ is antipodal to $\widehat{\boldsymbol{v}}_2$, i.e., $\widehat{\boldsymbol{v}}_1 = -\widehat{\boldsymbol{v}}_2$).

For the sake of simplification in the computation of the differential Slepian functions, the rotationally symmetric antipodal regions are rotated by $\pi-\varphi$ around z-axis and then by ϑ around y-axis such that the rotated regions $\tilde{R}_1$ and $\tilde{R}_2$ are centered at (rotationally symmetric around) the North ($\widehat{\boldsymbol{\eta}}$) and South poles of the unit sphere respectively as shown in Fig. 5(b). The regions are now *azimuthally* symmetric antipodal regions and form a special case of rotationally symmetric antipodal regions. Owing to the orientation of the azimuthally symmetric regions, the formulation of the differential Slepian concentration problem is significantly simplified. For the azimuthally symmetric region R_k, the formulation of ${}_kD_{\ell\ell'}^{mm'}$ is simplified by exploiting the orthogonality of complex exponentials along longitude such that

$$ {}_kD_{\ell\ell'}^{mm'} = 2\pi\delta_{mm'} \underbrace{\int_{\theta_{1k}}^{\theta_{2k}} Y_\ell^m(\theta,0)\overline{Y_{\ell'}^m(\theta,0)} \sin\theta d\theta}_{\triangleq {}_kD_{\ell\ell'}^m}, \ \ k=[1,2]. $$

Here $\theta_{11} = 0$ and $\theta_{22} = \pi$, whereas θ_{21} and θ_{12} represent the co-latitudinal radii for the rotated regions $\tilde{R}_1$ and $\tilde{R}_2$ respectively. The integral represented by ${}_kD_{\ell\ell'}^m$ can be evaluated analytically for all $\ell,\ell' \geq m$ as [23], [43]

$$ {}_kD_{\ell\ell'}^m = (-1)^m \frac{\sqrt{(2\ell+1)(2\ell'+1)}}{2} \sum_{q=|\ell-\ell'|}^{|\ell+\ell'|} \begin{pmatrix} \ell & q & \ell' \\ 0 & 0 & 0 \end{pmatrix} \times \begin{pmatrix} \ell & q & \ell' \\ m & 0 & -m \end{pmatrix} \Big(P_{q-1}^0(\cos\theta_{2k}) + P_{q+1}^0(\cos\theta_{1k}) - P_{q+1}^0(\cos\theta_{2k}) - P_{q-1}^0(\cos\theta_{1k}) \Big). \tag{41} $$

Here the arrays of indices are the Wigner-3j symbols [42]. Consequently, the coupling matrix $\boldsymbol{H}$ in (27) reduces to a block diagonal matrix of the form: $\boldsymbol{H} = \text{diag}(\boldsymbol{H}_0, \boldsymbol{H}_1, \boldsymbol{H}_1, \ldots, \boldsymbol{H}_L, \boldsymbol{H}_L)$. Here we can see that every submatrix $\boldsymbol{H}_m, m \neq 0$ appears twice because of the doubly degenerate angular order $\pm m$. Therefore, instead of solving the eigenvalue equation (27) of size L^2, we only solve a series of $(L-m)\times(L-m)$ harmonic domain eigenvalue problems of the form

$$ \boldsymbol{H}_m \boldsymbol{f}_m = \lambda \boldsymbol{f}_m \tag{42} $$

for each $m = 0, 1, \ldots, L-1$. The submatrix $\boldsymbol{H}_m$ is of the form

$$ \boldsymbol{H}_m = \begin{bmatrix} H_{mm} & \cdots & H_{m,L-1} \\ \cdots & \ddots & \cdots \\ H_{L-1,m} & \cdots & H_{L-1,L-1} \end{bmatrix}, \tag{43} $$

where every $H_{\ell\ell'} = {}_1D_{\ell\ell'}^m - {}_2D_{\ell\ell'}^m$ and the vector of spherical harmonic coefficients is given as

$$ \boldsymbol{f}_m = [f_m, \ldots, f_{L-1}]^T. \tag{44} $$

Once we obtain the differential Slepian functions for the azimuthally symmetric antipodal regions, they are rotated back to the original location by applying rotation operator $\mathcal{X}(\vartheta,\varphi)$ on each Slepian function that rotates the signal in a sequence of ϑ around y-axis and φ around z-axis. The spherical harmonic coefficients of the Slepian function f for azimuthally symmetric antipodal regions and the rotated Slepian functions $\mathcal{X}(\vartheta,\varphi)f$ for rotationally symmetric antipodal regions are related by [42]

$$ (\mathcal{X}(\vartheta,\varphi)f)_\ell^m = \sum_{m'=-\ell}^{\ell} X_{m,m'}^\ell(\vartheta,\varphi)\,(f)_\ell^{m'}, \tag{45} $$

where

$$ X_{m,m'}^\ell(\vartheta,\varphi) = e^{-im\vartheta} d_{m,m'}^\ell(\vartheta). \tag{46} $$

Here $d_{m,m'}^\ell$ denotes the Wigner-d function of degree ℓ and orders m, m' [42].

F. Weighted Slepian Concentration Problem on the Sphere

We present the weighted Slepian concentration problem by choosing the weighting function $h(\widehat{\boldsymbol{u}})$ to be real, non-negative and bounded by unity, that is,

$$ 0 \leq h(\widehat{\boldsymbol{u}}) \leq 1, \quad \forall\, \widehat{\boldsymbol{u}} \in \mathbb{S}^2, \tag{47} $$

and

$$ g(\widehat{\boldsymbol{u}}) = 1, \quad \forall\, \widehat{\boldsymbol{u}} \in \mathbb{S}^2. \tag{48} $$

This article has been accepted for publication in a future issue of this journal, but has not been fully edited. Content may change prior to final publication. Citation information: DOI 10.1109/TSP.2020.2983644, IEEE Transactions on Signal Processing

We note that the classical Slepian concentration problem is also a special case of the weighted concentration problem. However the latter is more flexible as the localization of the spatial domain distribution of the energy over some portion of the sphere can be controlled by judiciously choosing the weighting function $h(\widehat{\boldsymbol{u}})$. For the choice of the weighting function, the Rayleigh quotient (18) is solved by finding eigenvectors of the matrix $\boldsymbol{H}$ with entries given in (16). Since $\boldsymbol{H}$ is positive-semi definite and Hermitian by definition, all the eigenvalues of $\boldsymbol{H}$ are real and non-negative and the corresponding eigenvectors can be chosen as orthonormal. The eigenvalue decomposition of $\boldsymbol{H}$ yields L^2 real eigenvectors $\boldsymbol{f}_\alpha$ with corresponding eigenvalue λ_α for $\alpha = 1, 2, \ldots, L^2$, where we index the eigenvalues (or eigenvectors) such that $\lambda_1 \geq \lambda_2 \geq \ldots \geq \lambda_{L^2} \geq 0$. For each eigenvector $\boldsymbol{f}_\alpha$, we obtain the spatial domain eigenfunction $f_\alpha(\widehat{\boldsymbol{u}})$ which we refer to as weighted Slepian function. Eigenvalue λ_α serves as a measure of the energy of the weighted signal $\sqrt{h(\widehat{\boldsymbol{u}})} f_\alpha(\widehat{\boldsymbol{u}})$.

G. Properties of Weighted Slepian Functions

The weighted Slepian functions exhibit three-fold orthogonality. Firstly, since the eigenvectors are orthonormal, the eigenfunctions are orthonormal in $\mathcal{H}_L$ by isomorphism, that is,

$$\langle \boldsymbol{f}_\alpha, \boldsymbol{f}_\beta \rangle_{\mathbb{C}} = \langle f_\alpha, f_\beta \rangle = \delta_{\alpha\beta}. \tag{49}$$

Secondly, since the eigenvectors satisfy

$$\langle \boldsymbol{H}\boldsymbol{f}_\alpha, \boldsymbol{f}_\beta \rangle_{\mathbb{C}} = \boldsymbol{f}_\beta^H \boldsymbol{H} \boldsymbol{f}_\alpha = \lambda_\alpha \langle \boldsymbol{f}_\alpha, \boldsymbol{f}_\beta \rangle_{\mathbb{C}} = \lambda_\alpha \delta_{\alpha\beta}, \tag{50}$$

we have, by isomorphism, the following spatial domain orthogonality of the eigenfunctions with respect to a weighted spatial domain inner product

$$\langle f_\alpha, f_\beta \rangle_h \triangleq \int_{\mathbb{S}^2} h(\widehat{\boldsymbol{u}}) f_\alpha(\widehat{\boldsymbol{u}}) \overline{f_\beta(\widehat{\boldsymbol{u}})} ds(\widehat{\boldsymbol{u}}) = \lambda_\alpha \delta_{\alpha\beta}. \tag{51}$$

Finally, there is a third sense in which the eigenfunctions are orthogonal

$$\langle f_\alpha, f_\beta \rangle_{1-h} = (1 - \lambda_\alpha) \delta_{\alpha\beta}, \tag{52}$$

that is, with respect to the complementary weighted inner product. We further note that $\{f_\alpha/\sqrt{\lambda_\alpha}\}$ and $\{f_\alpha/\sqrt{1-\lambda_\alpha}\}$, for $\lambda_\alpha > 0$ are orthonormal with respect to the weighted inner product and complementary weighted inner product respectively.

IV. Applications: Spectral Estimation and Robust Modeling

In some applications, for instance, the reconstruction of the HRTF in acoustics [44] or spectral estimation in geophysics and cosmology [26] the measurements over a particular region on the sphere are unavailable, unreliable or subjected to large errors. To support these signal processing applications, Slepian functions have been used for signal extrapolation [45], localized spectral analysis and spectral estimation [24], [32]. Here we provide two applications of the proposed differential and weighted Slepian functions for localized spectral estimation and robust modeling of the signal on the sphere.

A. Estimation of Localized Energy Spectrum

The band-limited differential Slepian functions serve as a good choice for localization functions due to their optimal spatial concentration and orthogonality properties. For a global function $p \in L^2(\mathbb{S}^2)$, we obtain its localized version using the differential Slepian function $f(\widehat{\boldsymbol{u}})$ as

$$\Psi(\widehat{\boldsymbol{u}}) = f(\widehat{\boldsymbol{u}}) p(\widehat{\boldsymbol{u}}). \tag{53}$$

Using the background presented in Section II, we find the energy spectrum of the localized function $\Psi(\widehat{\boldsymbol{u}})$. We assume that the spherical harmonic coefficients of the function p are zero-mean random variables, and the energy spectrum only depends on ℓ (i.e., the function has isotropic energy spectrum). The global energy spectrum is given by

$$\mathbb{E}\left[(p)_\ell^m \overline{(p)_{\ell'}^{m'}} \right] = \frac{S_{pp}(\ell)}{2\ell+1} \delta_{\ell\ell'} \delta_{mm'}, \tag{54}$$

where $\mathbb{E}[\,\cdot\,]$ is the expectation operator. Let the localized energy spectrum be represented as $S_{\Psi\Psi}$. Using the theoretical framework presented in [26], [32], the relation between S_{pp} and the expected value of $S_{\Psi\Psi}$ is given by

$$\begin{aligned} \mathbb{E}\left[S_{\Psi\Psi}(\ell)\right] &\triangleq \sum_{m=-\ell}^{\ell} \mathbb{E}\left[(\Psi)_\ell^m \overline{(\Psi)_\ell^m} \right] \\ &= (2\ell+1) \sum_{q=0}^{L-1} S_{ff}(q) \sum_{r=|\ell-q|}^{\ell+q} S_{pp}(r) \begin{pmatrix} q & r & \ell \\ 0 & 0 & 0 \end{pmatrix}^2, \end{aligned} \tag{55}$$

where the quantity $\left(\begin{smallmatrix} q & r & \ell \\ 0 & 0 & 0 \end{smallmatrix}\right)$ represents the Wigner 3-j symbols [42].

To illustrate the effectiveness of the differential Slepian functions as the localization window functions, we estimate the white and red stochastic processes on the sphere. The energy spectrum of various stochastic processes follows the power law given by

$$S_{pp}(\ell) \sim \ell^{\epsilon}. \tag{56}$$

When the energy per angular degree is constant, i.e., for $\epsilon = 0$, the process is called a white process. If $\epsilon = -2$, we may refer to the process as a red process. The definition of these processes may vary from one application to another [26]. For the band-limit $L = 16$, and the regions R_1 and R_2 being taken as North and South polar caps of radii $\pi/6$ and $\pi/8$ respectively, the estimate of the energy spectrum for white and red process is plotted in Fig. 6 and Fig. 7. The estimates are obtained using the first 6 most concentrated window functions previously plotted in Fig. 1. It can be observed that the localized estimates approach the global spectra for both white and red processes. The spectral bias for low degrees $\ell < L$ is simply a consequence of the fact that the localized estimate of the spectrum is a smoothed version of the global spectrum (55). Each differential Slepian function $f(\widehat{\boldsymbol{u}})$, used in (53) for spatial localization, leads to a different estimate. Such single-taper estimates can be combined as a weighted sum to obtian a multi-taper spectral estimate analogous to the one proposed in [24], [26], [32], [46].

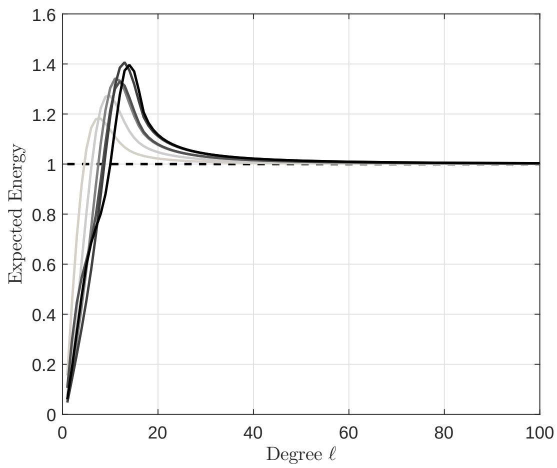

Fig. 6: Expected localized energy spectral density of a global white process using differential Slepian functions for $L = 16$. The dashed line represents the global white process ($\epsilon = 0$). The expectations of the localized spectra were obtained using the 6 Slepian functions previously shown in Fig. 1.

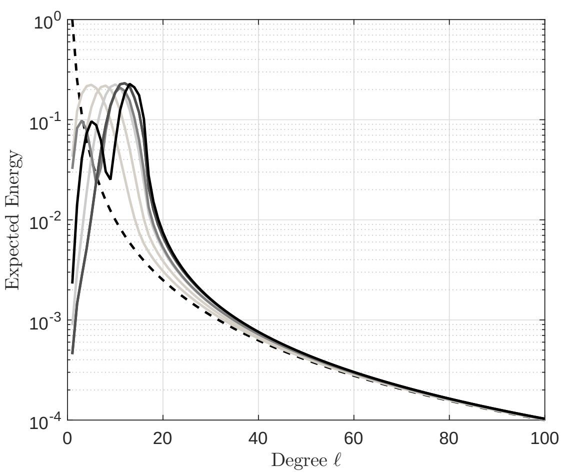

Fig. 7: Expected localized energy spectral density of a global red process using differential Slepian functions for $L = 16$. The dashed line represents the global red process ($\epsilon = -2$). The expectations of the localized spectra were obtained using the 6 Slepian functions previously shown in Fig. 1.

B. Robust Signal Modeling

Like the classical Slepian functions, the proposed weighted Slepian functions serve as alternative basis functions for the representation of the band-limited signal. Using the orthonormal weighted Slepian functions $\{f_\alpha(\widehat{\boldsymbol{u}})\}$, any bandlimited function $g \in \mathcal{H}_L$ can be expanded as

$$g(\widehat{\boldsymbol{u}}) = \sum_{\alpha=1}^{L^2} (g)_\alpha f_\alpha(\widehat{\boldsymbol{u}}) = \sum_{\alpha=1}^{L^2} \sqrt{\lambda_\alpha}\, (g)_{h:\alpha} f_\alpha(\widehat{\boldsymbol{u}}), \qquad (57)$$

where

$$(g)_\alpha \triangleq \langle g, f_\alpha \rangle, \quad (g)_{h:\alpha} \triangleq \langle g, f_\alpha/\sqrt{\lambda_\alpha} \rangle_h. \qquad (58)$$

Therefore, if the band-limited function g is determined from the local information implicit in the weighting function h, we can determine the coefficients of the band-limited function as

$$(g)_\alpha = \frac{1}{\sqrt{\lambda_\alpha}} \langle g, f_\alpha \rangle_h. \qquad (59)$$

For example with $h(\widehat{\boldsymbol{u}}) = I_R(\widehat{\boldsymbol{u}})$ (classical problem), the information about the function is available over the region R only. The energy associated with the α-th eigenfunction with respect to the weighted localized inner product is $|(g)_{h:\alpha}|^2$. However, this implies the energy on the sphere is $|(g)_{h:\alpha}|^2/\lambda_\alpha$. Therefore, we may see a significant growth in the energy on the sphere or significant enhancement of noise for small values of λ in the computation of $(g)_\alpha$ using (59).

V. Conclusions

In this work, we have presented a generalization of the Slepian concentration problem on the sphere by introducing weighting functions in the formulation of the problem. Assigning different values to the weighting functions, we have formulated the two variants: differential and weighted Slepian concentration problems of finding band-limited optimally concentrated functions on the sphere. The differential Slepian concentration problem takes into account two regions on the sphere and maximizes the energy concentration of a band-limited signal in one region while the energy is minimized in the other region. The weighted Slepian concentration problem uses non-negative weighting as a window function in the formulation for the localization of the signal energy. The solution of each problem yields eigenfunctions, referred to as Slepian functions, that serve as alternative basis functions for the representation of band-limited functions. We have also presented and analysed the properties of the proposed Slepian functions. Furthermore, we demonstrated the usefulness of the proposed Slepian functions for signal representation, localized spectrum estimation and signal modeling to support the applications in cosmology, geophysics, acoustics and beyond.

Appendix

A. Orthogonality of the Differential Slepian Functions

Proof. Using the definition of the differential Slepian functions:

$$\langle f_\alpha, f_\beta \rangle_{R_1} - \langle f_\alpha, f_\beta \rangle_{R_2} = \lambda_\alpha \langle f_\alpha, f_\beta \rangle_{\mathbb{S}^2}. \qquad (60)$$

If $\alpha = \beta$, then $\langle f_\alpha, f_\alpha \rangle_{R_2} \geq 0$ and $\langle f_\alpha, f_\alpha \rangle_{\mathbb{S}^2} = 1$, therefore (60) reduces to

$$\langle f_\alpha, f_\alpha \rangle_{R_1} \geq \lambda_\alpha. \qquad (61)$$

Say $\mathbb{S}^2 = R_1 + R_2 + R_*$, then for $\alpha \neq \beta$ we can rewrite (32) as

$$\langle f_\alpha, f_\beta \rangle_{R_1} + \langle f_\alpha, f_\beta \rangle_{R_2} + \langle f_\alpha, f_\beta \rangle_{R_*} = 0. \qquad (62)$$

Adding (60) and (62) we get

$$2 \langle f_\alpha, f_\beta \rangle_{R_1} = - \langle f_\alpha, f_\beta \rangle_{R_*}. \qquad (63)$$

Using the Cauchy-Schwarz inequality for $\langle f_\alpha, f_\beta \rangle_{R_*}$, we get

$$| \langle f_\alpha, f_\beta \rangle_{R_*} | \leq \sqrt{\langle f_\alpha, f_\alpha \rangle_{R_*}} \sqrt{\langle f_\beta, f_\beta \rangle_{R_*}}, \qquad (64)$$

This article has been accepted for publication in a future issue of this journal, but has not been fully edited. Content may change prior to final publication. Citation information: DOI 10.1109/TSP.2020.2983644, IEEE Transactions on Signal Processing

where

$$\begin{aligned}\sqrt{\langle f_\alpha, f_\alpha\rangle_{R_*}} &= \sqrt{\langle f_\alpha, f_\alpha\rangle_{\mathbb{S}^2} - \langle f_\alpha, f_\alpha\rangle_{R_1} - \langle f_\alpha, f_\alpha\rangle_{R_2}} \\ &\leq \sqrt{1 - \langle f_\alpha, f_\alpha\rangle_{R_1}} \\ &\leq \sqrt{1-\lambda_\alpha}. \end{aligned} \tag{65}$$

So (64) implies that $|\langle f_\alpha, f_\beta\rangle_{R_*}| \leq \sqrt{1-\lambda_\alpha}\,\sqrt{1-\lambda_\beta}$ and using this in (63) results in

$$|\langle f_\alpha, f_\beta\rangle_{R_1}| \leq \frac{1}{2}\sqrt{1-\lambda_\alpha}\,\sqrt{1-\lambda_\beta}. \tag{66}$$

To find the bound on the angle between two Slepian functions, we use (66) in the definiton of inner product as

$$|f_\alpha|_{R_1}|f_\beta|_{R_1}|\cos\gamma_{f_\alpha,f_\beta}| \leq \frac{1}{2}\sqrt{1-\lambda_\alpha}\,\sqrt{1-\lambda_\beta}. \tag{67}$$

Since

$$\lambda_\alpha = |f_\alpha|^2_{R_1} - |f_\alpha|^2_{R_2} \;\Rightarrow\; \lambda_\alpha \leq |f_\alpha|^2_{R_1}. \tag{68}$$

Then for positive eigenvalues, we can say $\sqrt{\lambda_\alpha} \leq |f_\alpha|_{R_1}$, or

$$\frac{1}{|f_\alpha|_{R_1}} \leq \frac{1}{\lambda_\alpha}. \tag{69}$$

Rearranging (67) and employing (69), we can prove that

$$|\cos\gamma_{f_\alpha,f_\beta}| \leq \frac{1}{2}\frac{\sqrt{1-\lambda_\alpha}\,\sqrt{1-\lambda_\beta}}{\sqrt{\lambda_\alpha}\,\sqrt{\lambda_\beta}} \qquad \lambda_{\alpha,\beta} > 0. \tag{70}$$

□

REFERENCES

[1] D. Slepian and H. O. Pollak, "Prolate spheroidal wave functions, Fourier analysis and uncertainity-I," *Bell Syst. Tech. J.*, vol. 40, pp. 43–63, Jan. 1961.

[2] H. J. Landau and H. O.Pollak, "Prolate spheroidal wave functions, Fourier analysis and uncertainity-II," *Bell Syst. Tech. J.*, vol. 40, pp. 65–84, Jan. 1961.

[3] D. Slepian, "Prolate spheroidal wave functions, Fourier analysis and uncertainity-IV: Extensions to many dimensions; generalized prolate spheroidal functions," *Bell Syst. Tech. J.*, vol. 43, pp. 3009–3057, 1964.

[4] H. J. Landau and H. O.Pollak, "Prolate spheroidal wave functions, Fourier analysis and uncertainity-III: The dimension of the space of essentially time- and band-limited signals," *Bell Syst. Tech. J.*, vol. 41, pp. 1295–1336, 1962.

[5] I. C. Moore and M. Cada, "Prolate spheroidal wave functions, an introduction to the slepian series and its properties," *Appl. and Computational Harmonic Anal.*, vol. 16, no. 3, pp. 208–230, 2004.

[6] J. A. Hogan and J. D. Lakey, *Duration and Bandwidth Limiting: Prolate Functions, Sampling, and Applications*. Springer Science & Business Media, 2011.

[7] R. S. Dilmaghani, M. Ghavami, B. Allen, and H. Aghvami, "Novel uwb pulse shaping using prolate spheroidal wave functions," in *Proc. 14th IEEE Personal, Indoor and Mobile Radio Commun., PIMRC 2003*, Sept. 2003, pp. 602–606.

[8] S. Haykin and D. J. Thomson, "Signal detection in a nonstationary environment reformulated as an adaptive pattern classification problem," *Proceedings of the IEEE*, vol. 86, no. 11, pp. 2325–2344, 1998.

[9] W. Xu and C. Chamzas, "On the extrapolation of band-limited functions with energy constraints," *IEEE Trans. Acoust., Speech and Signal Process.*, vol. 31, no. 5, pp. 1222–1234, 1983.

[10] L. Gosse, "Effective band-limited extrapolation relying on slepian series and ℓ_1 regularization," *Computers & Mathematics with Appl.*, vol. 60, no. 5, pp. 1259–1279, 2010.

[11] M. A. Davenport and M. B. Wakin, "Compressive sensing of analog signals using discrete prolate spheroidal sequences," *Appl. and Computational Harmonic Anal.*, vol. 33, no. 3, pp. 438–472, 2012.

[12] S. Şenay, J. Oh, and L. F. Chaparro, "Regularized signal reconstruction for level-crossing sampling using slepian functions," *Signal Process.*, vol. 92, no. 4, pp. 1157–1165, 2012.

[13] S. Şenay, L. F. Chaparro, and L. Durak, "Reconstruction of nonuniformly sampled time-limited signals using prolate spheroidal wave functions," *Signal Process.*, vol. 89, no. 12, pp. 2585–2595, 2009.

[14] R. Demesmaeker, M. G. Preti, and D. Van De Ville, "Augmented slepians: Bandlimited functions that counterbalance energy in selected intervals," *IEEE Trans. on Signal Process.*, vol. 66, no. 15, pp. 4013–4024, 2018.

[15] G. G. Walter and X. Shen, "Sampling with prolate spheroidal wave functions," *Sampling Theory in Signal and Image Process.*, vol. 2, no. 1, pp. 25–52, 2003.

[16] K. Khare and N. George, "Sampling theory approach to prolate spheroidal wavefunctions," *J. Phys. A: Math. and General*, vol. 36, no. 39, p. 10011, 2003.

[17] D. Cheng and K. I. Kou, "Novel sampling formulas associated with quaternionic prolate spheroidal wave functions," *Advances in Appl. Clifford Algebras*, vol. 27, no. 4, pp. 2961–2983, 2017.

[18] S. Şenay, L. F. Chaparro, M. Sun, and R. J. Sclabassi, "Compressive sensing and random filtering of eeg signals using slepian basis," in *Proc. 16th Eur. Signal Process. Conf., 2008*. IEEE, Aug. 2008, pp. 1–5.

[19] N. Hoogenboom, J.-M. Schoffelen, R. Oostenveld, L. M. Parkes, and P. Fries, "Localizing human visual gamma-band activity in frequency, time and space," *Neuroimage*, vol. 29, no. 3, pp. 764–773, 2006.

[20] B. R. Frieden, "Viii evaluation, design and extrapolation methods for optical signals, based on use of the prolate functions," in *Progress in Opt.* Elsevier, 1971, vol. 9, pp. 311–407.

[21] F. J. Simons and D. V. Wang, "Spatiospectral concentration in the cartesian plane," *GEM-Int. J. Geomathematics*, vol. 2, no. 1, pp. 1–36, 2011.

[22] A. Albertella, F. Sansò, and N. Sneeuw, "Band-limited functions on a bounded spherical domain: the Slepian problem on the sphere," *J. Geodesy*, vol. 73, no. 9, pp. 436–447, Jun. 1999.

[23] F. J. Simons, F. A. Dahlen, and M. A. Wieczorek, "Spatiospectral concentration on a sphere," *SIAM Rev.*, vol. 48, no. 3, pp. 504–536, 2006.

[24] M. A. Wieczorek and F. J. Simons, "Localized spectral analysis on the sphere," *Geophys. J. Int.*, vol. 162, no. 3, pp. 655–675, Sep. 2005.

[25] C. D. Beggan, J. Saarimäki, K. A. Whaler, and F. J. Simons, "Spectral and spatial decomposition of lithospheric magnetic field models using spherical slepian functions," *Geophys. J. Int.*, vol. 193, no. 1, pp. 136–148, 2013.

[26] F. A. Dahlen and F. J. Simons, "Spectral estimation on a sphere in geophysics and cosmology," *Geophys. J. Int.*, vol. 174, pp. 774–807, 2008.

[27] F. J. Simons and F. Dahlen, "Spherical slepian functions and the polar gap in geodesy," *Geophys. J. Int.*, vol. 166, no. 3, pp. 1039–1061, 2006.

[28] M. J. Evans, J. A. Angus, and A. I. Tew, "Analyzing head-related transfer function measurements using surface spherical harmonics," *J. Acoust. Soc. America*, vol. 104, no. 4, pp. 2400–2411, 1998.

[29] A. P. Bates, Z. Khalid, and R. A. Kennedy, "On the use of slepian functions for the reconstruction of the head-related transfer function on the sphere," in *Proc. 9th IEEE Int. Conf. Signal Process. Commun. Syst., ICSPCS 2015,*. IEEE, Dec. 2015, pp. 1–7.

[30] F. J. Simons, "Slepian functions and their use in signal estimation and spectral analysis," in *Handbook of Geomathematics*. Springer, 2010, pp. 891–923.

[31] A. Plattner and F. J. Simons, "Potential-field estimation using scalar and vector slepian functions at satellite altitude," *Handbook of Geomathematics*, pp. 2003–2055, 2014.

[32] M. A. Wieczorek and F. J. Simons, "Minimum variance multitaper spectral estimation on the sphere," *J. Fourier Anal. Appl.*, vol. 13, no. 6, pp. 665–692, 2007.

[33] L. Longuevergne, B. R. Scanlon, and C. R. Wilson, "Grace hydrological estimates for small basins: Evaluating processing approaches on the high plains aquifer, usa," *Water Resources Research*, vol. 46, no. 11, 2010.

[34] M. Tsitsvero, S. Barbarossa, and P. Di Lorenzo, "Signals on graphs: Uncertainty principle and sampling," *IEEE Trans. Signal Process.*, vol. 64, no. 18, pp. 4845–4860, 2016.

[35] D. Van De Ville, R. Demesmaeker, and M. G. Preti, "When slepian meets fiedler: Putting a focus on the graph spectrum," *IEEE Signal Process. Lett.*, vol. 24, no. 7, pp. 1001–1004, 2017.

[36] R. Liégeois, I. Merad, and D. Van De Ville, "Time-resolved analysis of dynamic graphs: an extended slepian design," in *Wavelets and Sparsity XVIII*, vol. 11138. International Society for Optics and Photonics, 2019, p. 1113810.

[37] M. Petrović and D. Van De Ville, "Slepian guided filtering of graph signals," in *Wavelets and Sparsity XVIII*, vol. 11138. International Society for Optics and Photonics, 2019, p. 111380D.

[38] A. P. Bates, Z. Khalid, and R. A. Kennedy, "Efficient computation of slepian functions for arbitrary regions on the sphere," *IEEE Trans. Signal Process.*, vol. 65, no. 16, pp. 4379–4393, 2017.

[39] F. J. Simons, J. C. Hawthorne, and C. D. Beggan, "Efficient analysis and representation of geophysical processes using localized spherical basis functions," in *Wavelets XIII*, vol. 7446. International Society for Optics and Photonics, 2009, p. 74460G.

[40] F. J. Simons and A. Plattner, "Scalar and vector slepian functions, spherical signal estimation and spectral analysis," in *Handbook of Geomathematics: Second Edition*. Springer Berlin Heidelberg, 2015, pp. 2563–2608.

[41] A. P. Bates, Z. Khalid, and R. A. Kennedy, "Slepian spatial-spectral concentration problem on the sphere: Analytical formulation for limited colatitude–longitude spatial region," *IEEE Trans. on Signal Process.*, vol. 65, no. 6, pp. 1527–1537, 2016.

[42] R. A. Kennedy and P. Sadeghi, *Hilbert Space Methods in Signal Processing*. Cambridge, UK: Cambridge University Press, Mar. 2013.

[43] Z. Khalid, R. A. Kennedy, and J. D. McEwen, "Slepian spatial-spectral concentration on the ball," *Appl. and Computational Harmonic Anal.*, vol. 40, no. 3, pp. 470–504, 2016.

[44] A. P. Bates, Z. Khalid, and R. A. Kennedy, "Novel sampling scheme on the sphere for head-related transfer function measurements," *IEEE/ACM Trans. on Audio, Speech and Lang. Process. (TASLP)*, vol. 23, no. 6, pp. 1068–1081, 2015.

[45] Y. Alem, Z. Khalid, and R. A. Kennedy, "Band-limited extrapolation on the sphere for signal reconstruction in the presence of noise," in *Proc. IEEE Int. Conf. Acoust., Speech and Signal Process., ICASSP'2014*, Florence, Italy, May 2014, pp. 4169–4173.

[46] D. J. Thomson, "Spectrum estimation and harmonic analysis," *Proceedings of the IEEE*, vol. 70, no. 9, pp. 1055–1096, 1982.